Association of Terminal Complement Proteins in Solution and Modulation by Suramin[†,‡]

Cristian Saez,[§] Nicole M. Thielens,[||] Edward S. Bjes,[§] and Alfred F. Esser*[,§]

Division of Cell Biology and Biophysics, School of Biological Sciences, University of Missouri−Kansas City, Kansas City, Missouri 64110, and Laboratoire d'Enzymologie Moléculaire, Institut de Biologie Structurale Jean-Pierre Ebel, F-38027 Grenoble Cedex 1, France

Received January 7, 1999; Revised Manuscript Received March 25, 1999

ABSTRACT: The association of terminal complement proteins was investigated by analytical ultracentrifugation and multi-angle laser light scattering. Native C8 and C9 formed a heterodimer in solution of physiological ionic strength with a free-energy change $\Delta G°$ of −8.3 kcal/mol and a dissociation constant K_d of 0.6 μM (at 20 °C) that was ionic strength- and temperature-dependent. A van't Hoff plot of the change in K_d was linear between 10 and 37 °C and yielded values of $\Delta H° = -12.9$ kcal/mol and $\Delta S° = -15.9$ cal mol^{-1} deg^{-1}, suggesting that electrostatic forces play a prominent role in the interaction of C8 with C9. Native C8 also formed a heterodimer with C5, and low concentrations of polyionic ligands such as protamine and suramin inhibited the interaction. Suramin induced high-affinity trimerization of C8 ($K_d = 0.10$ μM at 20 °C) and dimerization of C9 ($K_d = 0.86$ μM at 20 °C). Suramin-induced C8 oligomerization may be the primary reason for the drug's ability to prevent complement-mediated hemolysis. Analysis of sedimentation equilibria and also of the fluorescence enhancement of suramin when bound to protein provided evidence for two suramin-binding sites on each C9 and three on each C8 in the oligomers. Oligomerization could be reversed by high suramin concentrations, but 8-aminonaphthalene-1,3,6-trisulfonate ($ANTS^{2-}$), which mimics half a suramin molecule, could not compete with suramin binding and oligomerization suggesting that the drug also binds nonionically to the proteins.

The reversible interaction between the five terminal complement proteins[1] C5, C6, C7, C8, and C9 in solution (*1*) provided the first indication for possible arrangements of these proteins in the membrane attack complex (MAC)[2] of complement. Thus, it is now known that at half-physiological ionic strength these proteins can form a pentameric C5,6,7,8,9 complex when all proteins are mixed together in solution. However, only C8−C9, C8−C5, C5−C6, and C5−C7 dimers were observed when individual pairs of these proteins were mixed, which inspired the proposal that in the MAC the proteins were arranged in the following manner:

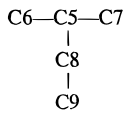

These studies were corroborated and extended by Sodetz and co-workers (*2*) who established that the C8β and C8α subunits mediate binding of C8 to C5b-7 and C9 to C5b-8, respectively, and provided evidence that there is only one binding site on soluble C8 for C9 (*3*). In addition, Bhakdi and Tranum-Jensen (*4*) demonstrated that at low temperatures only one C9 molecule would bind to one C5b-8 complex on a membrane, despite the potential for the incorporation of up to six C9 molecules in the membrane-bound MAC (*5*). The interaction sites on these proteins are unknown, but the presence of three cysteine-rich domains at identical locations in the different primary sequences of these proteins generated the idea that they serve as protein−protein contact sites or "molecular fasteners" in the assembly of the MAC (*6*). This hypothesis was reinforced by the observation that polyionic substances such as suramin, heparin, or protamine inhibited the self-aggregation of C9 into a tubular structure called poly(C9) as well as the binding of the individual proteins to their cognate membrane-bound complexes (*7*). Since the same polyionic substances were known to inhibit binding of LDL particles to the LDL receptor (*8*), the corresponding domain in C9 became the primary candidate for a contact site in the assembly of the MAC (*9*). Tschopp and co-workers (*7*, *10*) developed a model (Figure 1) which proposes that within folded C9 there are three ionic interaction sites in the native protein (marked 1, 2, and 3 in the figure) one of which (number 2) is the sequence D101-D111 within the cysteine-rich LDL receptor domain. Two of them are cryptic but become unmasked and guide the assembly process by

[†] The research reported here was supported by NIH grants R01-AI 19478 and GM 53748 and the Marion Merrell Dow Professorship Endowment to A. F. E.

[‡] Dedicated to Professor Rainer Jaenicke on the occasion of his retirement.

* To whom correspondence should be addressed.

[§] University of Missouri−Kansas City.

[||] Institut de Biologie Structurale Jean-Pierre Ebel.

[1] Complement proteins are named in accordance with recommendations in *Bulletin World Health Organization* (1968) *39*, 935.

[2] Abbreviations: $ANTS^{2-}$, 8-aminonaphthalene-1,3,6-trisulfonate; bis-ANS^{2-}, bis (1,8-anilinonaphthalenesulfonate); DSC, differential scanning calorimetry; MAC, membrane attack complex of complement; MALLS, multi-angle laser light scattering; Mops, 3-(*N*-morpholino)-1-propanesulfonic acid; s*, apparent sedimentation coefficient; rms, root-mean-square error.

10.1021/bi990040j CCC: $18.00
Published on Web 05/06/1999

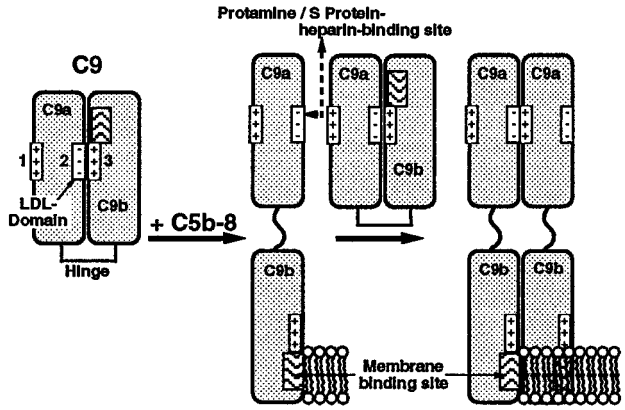

FIGURE 1: Proposed model of C9 interaction with C5b-8, polymerization, and insertion into a membrane (modified from ref *10*).

combining with a site on the surface of another C9 (marked as site 1). In addition there is a protected hydrophobic patch in the folded protein that inserts into the target membrane when C9 refolds during MAC assembly. It was proposed specifically that cationic reagents such as protamine or a basic peptide representing the heparin-binding site of S-protein/vitronectin bind to site 2, and by inference, anionic substances such as heparin or suramin bind to site 3 during the assembly process.

Because it was unclear whether inhibition of MAC assembly by the polyions involved the primary or the secondary (cryptic) sites, or both, we decided to investigate their influence on the interactions between pairs of these proteins in solution. We also wanted to determine the relative affinities between these proteins at physiological ionic strength and the nature of the inhibitory action of suramin. This drug, a bis-hexasulfonated naphthylurea also known as Germanin or Bayer 205, was developed by the Bayer company between 1910 and 1920 to treat trypanosomiasis and was shown later to inhibit complement activity (*11*). In recent years suramin has been also tested in AIDS therapy (*12*) and as an anticancer agent (*13*). Its specific interaction with proteins such as acidic fibroblast growth factor (*14*), neutrophil proteinases (*15*), and phosphoglycerate kinase (*16*) was investigated by others while our own studies using neutron scattering provided evidence that suramin produces C9 dimers (*17*). In the present study, sedimentation equilibrium centrifugation was used to determine the affinity between C8 and C9 and suramin. It is found that at physiological ionic strength suramin causes efficient formation of C9 dimers and C8 trimers, respectively, with affinity higher than that between the C8 and C9 molecules.

EXPERIMENTAL PROCEDURES

Reagents. All buffer components were of reagent grade. Suramin (hexasodium *sym*- bis [*m*-aminobenzoyl-*m*-amino-*p*-methylbenzoyl-1-aminonaphthalene-4,6,8-trisulfonate]carbamide) was kindly provided by the Bayer Co., and concentrations were estimated spectrophotometrically using an absorption coefficient of $\epsilon_{315} = 2.15 \times 10^4$ M^{-1} cm^{-1} (*18*). The suramin-related compounds, 8-aminonaphthalene-1,3,6-trisulfonate (disodium salt) ($ANTS^{2-}$) and bis-(1,8-anilinonaphthalenesulfonate) (bis-ANS^{2-}), were purchased from Molecular Probes, Inc. (Eugene, OR).

Proteins. Human C8 and C9 were purified from Cohn fraction III (Cutter Laboratories, Berkeley, CA) as published (*19*). Concentrations of C8 and C9 solutions were based on absorption coefficients of $\epsilon_{280} = 2.23 \times 10^5$ and 6.81×10^4 M^{-1} cm^{-1}, respectively (*19*). Human C5 was kindly provided by Dr. J. Janatova (Salt Lake City, UT). Radioiodinated C9 or C5, used in sucrose density gradient experiments, was prepared using the Iodo-beads procedure as recommended by the manufacturer (Pierce Chemical Co., Rockford, IL).

Fluorescence Measurements. All fluorescence measurements were made using an Aminco-Bowman II spectrofluorimeter (SLM Instruments, Urbana, IL) at 2−8 nm spectral excitation and emission resolution. All protein-fluorophore solutions were made up in 10 mM Mops, 0.15 M NaCl, pH 7.2, in a 5 mm microcuvette, and spectra were recorded at 20 °C. Since suramin has an enhanced fluorescence intensity when excited at 315 nm in the presence of C8 or C9, its affinity to C8 or C9 was examined by adding increasing concentrations of protein to a constant concentration of suramin. The stoichiometry and dissociation constants were calculated by a nonlinear least-squares fit of the fluorescence data according to the following relationship (*20*):

$$\Delta F = \Delta F_{max}\{(n[\text{protein}]_o + K_d) - (n[\text{protein}]_o - [\text{suramin}]_o + K_d)^2 - 4n[\text{protein}]_o[\text{suramin}]_o)^{1/2}\}/2[\text{suramin}]_o \quad (1)$$

where n is the suramin−protein-binding stoichiometry and $\Delta F = F - F_o$, where F and F_o are the fluorescence intensities in the presence and absence of protein, respectively. $\Delta F_{max} = F_{max} - F_o$, where F_{max} is the fluorescence intensity in the presence of saturating concentrations of the protein. The total concentrations of protein and suramin are designated $[\text{protein}]_o$ and $[\text{suramin}]_o$, respectively.

Sucrose Density Gradient Centrifugation. Evidence for the association of C8 with C5 or with C9 and for the effect of polyionic substance was obtained by ultracentrifugation in 10−20% (w/w) linear sucrose gradients as described by Stewart and Sodetz (*3*). In brief, ^{125}I-C9 or ^{125}I-C5 was incubated with 3-fold molar excess of unlabeled C8 in buffer (either 150 mM NaCl, 10 mM Tris, or 30 mM NaCl, 10 mM Tris, pH 7.2) and applied to sucrose density gradients prepared from the same buffers. Inhibitors were included in the gradient buffers at the indicated concentration. Centrifugation was performed at 4 °C, and gradients were fractionated from the top and the fractions analyzed for radioactivity.

Analytical Ultracentrifugation. Sedimentation equilibrium analysis was performed at different temperatures and rotor speeds using a Beckman XL-A ultracentrifuge. Solutions of the individual proteins and mixtures were loaded into six-channel 12 mm path length centerpieces. The protein radial distribution in each channel was determined by consecutive automated absorbance scans acquired at each 0.01 mm of radial spacing. Sedimentation data were analyzed by nonlinear least-squares methods (*20*) using different models running under SigmaPlot software (SPSS, Inc.). Data sets were collected after reaching thermodynamic equilibrium, judged to be achieved by the absence of systematic deviations in the plot of the difference between successive scans taken

12 h apart. Single-component sedimentation data were fit to the following:

$$c_r = c_0 \exp[\sigma(r^2 - r_0{}^2/2] + \text{base} \quad (2)$$

where c_r is the concentration of the solute at arbitrary radial position r, and c_0 at the reference radial position, r_0, and base is an error term for the nonsedimenting material. The parameter σ is the reduced molecular weight, and it is defined as the following:

$$\sigma = M_w(1 - \bar{V}\rho)\omega^2/RT \quad (3)$$

where R is the universal gas constant, T is the Kelvin temperature, ω is the rotor angular velocity, $\bar{V}$ is the protein partial specific volume, ρ is the solvent density, and M_w is the estimated molar mass of the individual proteins and complexes. The partial specific volumes, $\bar{V}$, of C8 and C9 were calculated to be 0.7203 and 0.7237 mL/g, respectively, using the program SEDNTERP that is available from http://biochem.uthscsa.edu/auc/xla2.html. Adjustments for temperature differences were calculated using the following relationship (*22*):

$$\bar{V}_T = \bar{V}_{25} + (4.25 \times 10^{-4})(T - 298.15) \quad (4)$$

where $\bar{V}_T$ is the partial specific volume at temperature T (in Kelvin) and $\bar{V}_{25}$ is the partial specific volume at 25 °C. The solvent density, ρ, was taken as 1.006 at 20 °C (*23*).

Nonlinear regression analysis of the sedimentation data using appropriate mathematical models was used to determine dissociation constants. In this case the protein concentration gradients were expressed as the sum of the distributions of the individual components and their reversible complex forms:

$$c_r = \sum_{i=1}^{n} c_{0,i} \exp[\sigma_i(r^2 - r_0^2/2] + \text{base} \quad (5)$$

The dissociation constant, K_d, for the C8−C9 interaction is defined as the following:

$$K_d = [C8][C9]/[C8{-}C9] \quad (6a)$$

and can be expressed in terms of the absorbance values in the centrifuge cell according to:

$$K_d' = A_{C8}A_{C9}/A_{C8-C9} \quad (6b)$$

and thus:

$$K_d = K_d'(\epsilon_{C8} + \epsilon_{C9})/\epsilon_{C8}\epsilon_{C9}L \quad (6c)$$

where L is the path length (1.2 cm) of the ultracentrifuge cell, ϵ_{C8} and ϵ_{C9} are the molar absorption coefficients of C8 and C9, respectively, and $\epsilon_{C8} + \epsilon_{C9}$ is the molar absorption coefficient of the complex which is assumed to be identical to the sum of the absorption coefficients of the individual proteins. The experimental data in the form of absorbance values as a function of cell radius were fitted to:

$$A_r = A_{0,C8} \exp[\sigma_{C8}(r^2 - r_0^2)/2] + A_{0,C9} \exp[\sigma_{C9}(r^2 - r_0^2)/2] + (1/K_d')A_{0,C8}A_{0,C9} \exp[\sigma_{C8-C9}(r^2 - r_0^2)/2] + \text{base} \quad (7)$$

where K_d', $A_{0,C8}$, $A_{0,C9}$, and base are fitting parameters (*24*).

In general, the dissociation constant, K_d, for oligomeric protein self-association in the presence of suramin can be defined as:

$$K_d = K_{d1}\,K_{d2}\cdots K_{dn-1} = [\text{Monomer}]_n/[\text{Monomer}]^n \quad (8a)$$

assuming that all components of the complex bind simultaneously. Thus:

$$K_d' = A^n{}_{\text{monomer}}/A_{n-\text{mer}} \quad (8b)$$

and the equilibrium constants were estimated as described by Lewis et al. (*24*) according to:

$$A_r = A_{0,\text{monomer}} \exp[\sigma_{\text{monomer}}(r - r_o{}^2)/2] + (1/K_d')A^n{}_{o,\text{monomer}} \exp[n\sigma_{\text{monomer}}(r - r_o{}^2)/2] + \text{base} \quad (9)$$

To obtain the correct protein absorbance at 280 nm, one must correct the experimental A_{280} values for the suramin absorption. Therefore, cells were also scanned at 314 nm where the protein absorbance is negligible, and experimental A_{280} values were corrected by subtracting a value of $(1.1)A_{314}$ at each radial distance since the suramin contribution is 1.1-fold higher at 280 nm than at 314 nm. Protein−suramin-binding stoichiometries were determined using plain buffer in the reference cell and resolving for protein monomer and oligomer absorbance contributions by radial decomposition of eq 2.

The equilibrium constants obtained under different temperature conditions were analyzed using the van't Hoff relation

$$\ln K = \Delta S°/R - (1/T)(\Delta H°/R) \quad (10)$$

Provided a plot of ln K versus $1/T$ (van't Hoff plot) is linear, the enthalpy and entropy changes of the reaction can be obtained from the slope and intercept, respectively.

Multi-Angle Laser Light Scattering. A DAWN model DSP-F light-scattering photometer (Wyatt Technology, Santa Barbara, CA) with a laser of wavelength 633 nm was used. The principles and operation of this instrument have been described elsewhere (*25*). Freshly chromatographed (Superdex 200, Pharmacia) C9 or C8 was diluted immediately with 10 mM Mops, 150 mM NaCl buffer, pH 7.2, in scintillation vials to a total volume of 4 mL and analyzed for light-scattering intensity. Because our instrument cannot be thermostated, all measurements were taken after thermal equilibrium was reached at about 27 ± 0.5 °C. Data were analyzed to determine the weight-average molecular weights (M_w) of different samples using the Wyatt ASTRA software (*25*). In the calculations we used specific refractive index increment (dn/dc) values of 0.19 and 0.18 for C9 and C8, respectively, that were previously determined using a differential refractometer (Optilab DSP; Wyatt Technology) operating at 633 nm.

Calorimetry. Calorimetric measurements were performed on a MC-2 differential scanning calorimeter (Microcal,

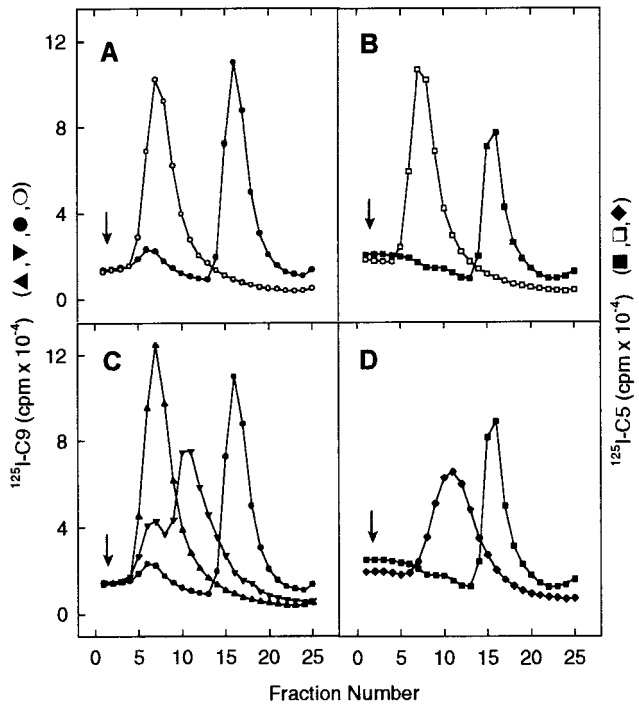

FIGURE 2: Sucrose density gradient centrifugation of C9−C8 and C5−C8 complexes. C8 mixed with ^{125}I−C9 (panels A, C) or with ^{125}I−C5 (panels B, D) was centrifuged in linear 10−20% sucrose density gradients prepared in either 30 mM NaCl (filled symbols) or 150 mM NaCl (open symbols) buffer. The sedimentation profile of each mixture in the presence of 20 μM (▼) or 200 μM suramin (▲) or 20 μg/mL protamine (◆) is shown in panels C and D. The arrows indicate the top of the gradients.

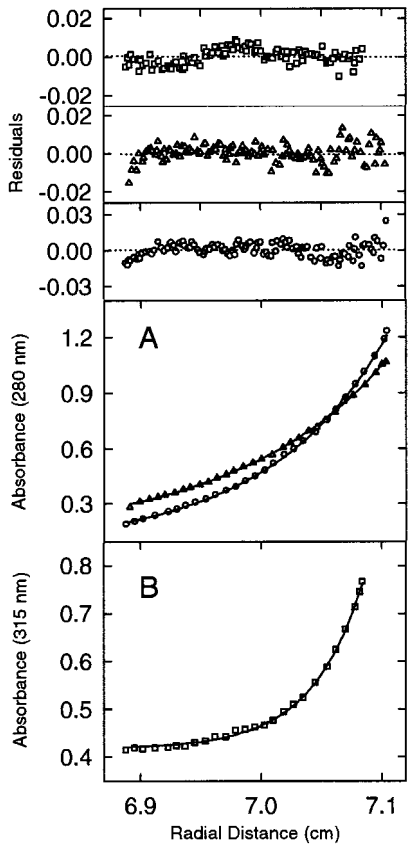

FIGURE 3: Sedimentation equilibrium centrifugation of an equimolar mixture of C8 and C9. (A) Sedimentation equilibrium data for C8 and C9 in 10 mM Mops, 0.15 M NaCl, pH 7.2 (○), and in 10 mM Mops, 0.3 M NaCl, pH 7.2 (△) are shown as absorbance at 280 nm versus radial position. The line drawn through the data points reflects a species of best-fit mass equal to 200 kDa (○) or a mixture of 150 and 71 kDa (△). (B) The effect of 20 μM suramin on sedimentation of the C8−C9 complex is shown as absorbance at 315 nm versus radial distance (□), and the line reflects a predominant species with a best-fit mass of 450 kDa. Only every third data point is shown to improve clarity, but all data points are shown for the distribution of residuals (the unweighted difference between the fitted and the experimental data) in the top panels. The protein concentration was 2 μM each, and the samples were centrifuged in a Beckman model XL-A at 8000 rpm and 20 °C for 24 h.

Northhampton, MA) using C8 at 20−25 μM. The solvent was 10 mM Mops, 150 mM NaCl, pH 7.2, buffer, and the heating rate was 30 °C/h. All thermograms were corrected for the instrumental baseline obtained by filling both cells with the buffer.

RESULTS

Interactions between Terminal Complement Proteins in Solution. Sucrose density gradient centrifugation had been used previously (*1*, *3*) to demonstrate interaction between terminal complement proteins in solution at half physiological ionic strength. By using this technique, we could now show that association between C8 and C5 and between C8 and C9 is blocked by polyionic substances such as suramin (Figure 2C) and protamine (Figure 2D). Suramin also inhibited C5−C8 complex formation, and protamine had a similar effect on C8−C9 interaction (not shown). Inhibition of heterodimer formation was dependent on inhibitor concentration (Figure 2C) but not on the charge of the inhibitor since both the anionic suramin and the cationic protamine were effective. Clearly, these polyionic ligands block not only the interactions between terminal complement proteins during MAC assembly on membranes (*7*) but also interactions among native proteins in solution. Because heterodimer formation was sensitive to ionic strength (Figure 2A,B), it was important to demonstrate their presence also at physiological conditions. Analytical sedimentation equilibrium centrifugation could be used to show molecular association of these proteins at normal physiological ionic strength, but no interaction was apparent when the ionic strength was raised to 0.3 M (Figure 3A). In buffered physiological saline and at 20 °C, native C8 and C9 interacted with a dissociation constant K_d of 0.59 ± 0.08 μM which increased to 3.4 ± 0.45 μM at 37 °C (Table 1). No significant C8 or C9 self-association was detected, and nonideal effects were negligible. At low ionic strength (0.05 M NaCl), some C8 aggregation could be detected (not shown).

Analysis of the sedimentation behavior of an equimolar mixture of C8 and C9 in the presence of suramin indicated that a bigger complex with an estimated mass of 450 kDa was present (Figure 3B). Since it was known from previous studies (*7*) that suramin inhibits C8−C9 association, the effect of suramin on each protein was analyzed individually to assess changes in their solution states. As shown in Figure 4A, suramin caused self-association of both proteins, C8 forming mostly a trimer and C9 a dimer at about a 5-fold molar excess of the drug which disappeared at salt concentrations higher than 0.2 M (Figure 4B). Modeling the protein equilibrium distribution resulted in a monomer−oligomer

Table 1: Summary of Sedimentation Equilibrium Results

protein	buffer composition	M_w[a]	K_d (μM)
C8	0.01 M Mops, 0.15 M NaCl, pH 7.2	155000	
C9	0.01 M Mops, 0.15 M NaCl, pH 7.2	71000	
C8 + C9	0.01 M Mops, 0.15 M NaCl, pH 7.2	200000	0.35 ± 0.06[b]
			0.59 ± 0.08[c]
			3.4 ± 0.45[d]
	0.01 M Mops, 0.30 M NaCl, pH 7.2	155000/ 71000	
	0.01 M Mops, 0.15 M NaCl, pH 7.2, 20 μM suramin	450000	
C8	0.01 M Mops, 0.15 M NaCl, pH 7.2, 10 μM suramin	450000	0.10 ± 0.02[b]
			0.11 ± 0.03[c]
			4.7 ± 0.25[d]
	0.01 M Mops, 0.65 M NaCl, pH 7.2, 10 μM suramin	155000	
C9	0.01 M Mops, 0.15 M NaCl, pH 7.2, 10 μM suramin	135000	0.16 ± 0.05[b]
			0.87 ± 0.17[e]
			48.3 ± 6.5[d]
	0.01 M Mops, 0.65 M NaCl, pH 7.2, 10 μM suramin	71000	

[a] The weight-average molecular weight of the predominant species as formed in the indicated buffer was calculated using eq 2. [b] Data were acquired at 12 °C. [c] Data were acquired at 20 °C. [d] Data were acquired at 37 °C.

dissociation constant K_d of 0.87 ± 0.17 μM for C9 and a K_d of 0.11 ± 0.03 μM for the C8 oligomer (Figure 5A). The molecular weights of the predominant species formed under these different conditions and their respective K_d values are summarized in Table 1. The formation of C8 oligomers in the presence of suramin was also examined by sedimentation velocity centrifugation at 35 000 rpm. The results (data not shown) indicated that the bulk of the protein sedimented with a *s** rate of 12 S, but most importantly, no loss of protein was detectable after overnight re-equilibration at 0 *g* force, indicating that large, pelletable oligomers were not formed.

Thermodynamic Analysis of C8−C9 and Self-Association Reactions. The nature of specific protein interactions can be deduced sometimes by analyzing the thermodynamics of the reactions. Therefore, we performed sedimentation experiments in the range of 8−37 °C and from the temperature dependence of the equilibrium constant for each complex (Figure 6) obtained the relevant $\Delta H°$, $\Delta S°$, and $\Delta G°$ values (Table 2). Because the van't Hoff plot for C8 trimer formation was biphasic, we used only the low-temperature portion of the plot (Figure 6B, solid line) in the calculations. The Gibbs standard free energy is similar for all three processes, the association of C8 and C9 as well as the suramin-induced self-association of C8 and C9, respectively. Of note, however, is the relatively high negative entropic contribution in the suramin-mediated multimer formation and the negative enthalpy of the associations. These values suggest that electrostatic interactions (*26*) are important in all three reactions.

Structural Analyses of Suramin−Protein Complexes. Suramin's structural features suggested that the observed protein dimer and trimer formation could be related to the molecule's symmetrical distribution of charges and/or hydrophobic aromatic rings. Two compounds, $ANTS^{2-}$ and bis-ANS^{2-}, appeared to be good suramin analogues to test this possibility since the former contains only a single trisulfonate group whereas the latter mimics the bivalent nature of suramin (Figure 7). Bis-ANS^{2-} caused C9 dimer and C8

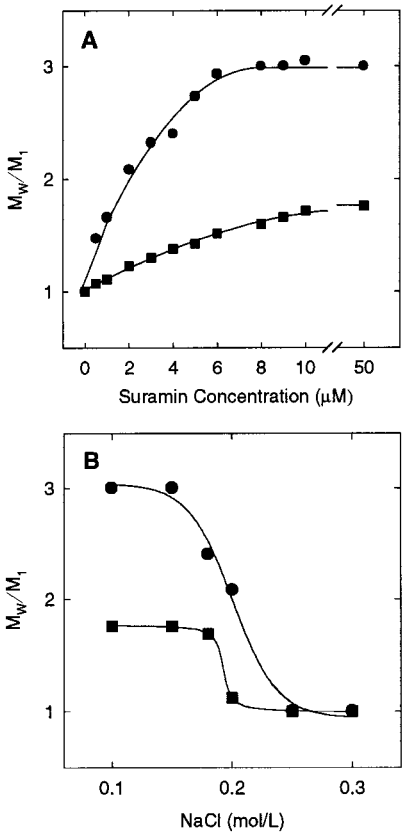

FIGURE 4: Suramin-dependent formation of C8 and C9 multimers. Formation of trimeric C8 and dimeric C9 (presented as M_w/M_1, where M_1= 150 000 for C8 (●) or M_1= 71 000 for C9 (■) and M_2 = best-fit mass of the predominant species) as a function of suramin concentration (A) and as a function of salt concentration at constant 10 μM suramin (B). Sedimentation equilibrium centrifugation of C8 was performed at 8000 rpm and C9 at 14000 rpm. All data were acquired at 20 °C, and the protein concentration was 2 μM.

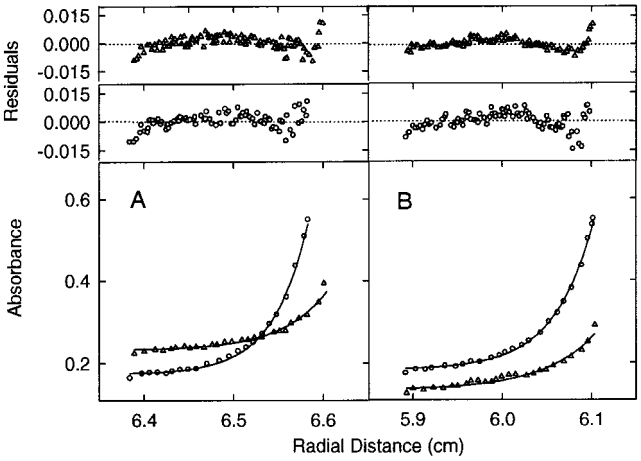

FIGURE 5: Self-association of C8 and C9 by suramin and bis-ANS^{2-}. (A) Sedimentation equilibrium data for C8 (○) and C9 (△) in the presence of 10 μM suramin recorded at 315 nm and (B) in the presence of 10 μM bis-ANS^{2-} recorded at 390 nm. The residuals of the fitted data for both proteins are plotted in the upper panels with each data point shown, whereas every third is indicated in the lower panels. Sedimentation equilibrium centrifugation of C8 was performed at 8000 rpm and C9 at 14000 rpm. All data were acquired at 20 °C, and the protein concentration was 2 μM.

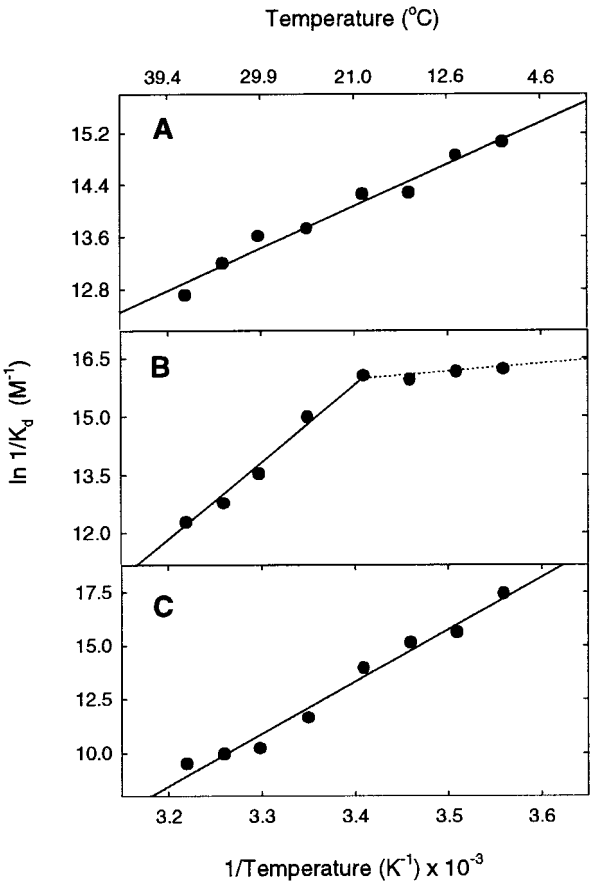

FIGURE 6: van't Hoff representation of the dissociation constants for the C8−C9 heterodimer (A) and the suramin-induced C8 trimer (B) and C9 dimer (C). The solid lines represent best linear fits of the data from which thermodynamic parameters were obtained.

Table 2: Thermodynamic Values for C8−C9 Interaction and Suramin-Mediated Self-Association of C8 and C9

reaction	$\Delta H°$ (kcal/mol)[a]	$\Delta S°$ (cal mol^{-1} deg^{-1})[a]	$\Delta G°$ (kcal/mol)[b]	rms[c]
[C8 + C9 ⇌ C8−C9]	−12.90	−15.94	−8.34	0.150
[3 C8 ⇌ C8$_3$]	−2.83[d]	−21.97[d]	−9.33	0.083
	−41.33[e]	−109.06[e]		0.205
[2 C9 ⇌ C9$_2$]	−48.31	−137.88	−8.13	0.492

[a] Calculated from Figure 6 using eq 10. [b] Calculated at 20 °C. [c] Square root of the variance fitting the van't Hoff plot. [d] Low-temperature limb of the van't Hoff plot. [d] High-temperature limb of the van't Hoff plot.

trimer formation just like suramin (Figure 5B), but ANTS^{2-} had no effect on the monomeric state of the proteins and it did not prevent suramin-induced oligomerization when present in excess over suramin (not shown).

Fluorescence spectroscopy was used to examine the protein environment to which suramin binds. Middaugh and colleagues (*14*) have reported that binding of suramin to growth factor proteins enhances its fluorescence significantly, suggesting that it resides in a less polar environment. Fluorescence enhancement (ΔF) of a fixed concentration of suramin (10 μM) elicited by C8 or C9 and calculated as described in the Methods section increased until a suramin/drug ratio of 2:3 was reached (Figure 8A). The experiments with C9 were performed at 4 °C to maximize dimer formation, while C8 titrations were done at room temperature. In panels B and C of Figure 8, we show the actual fluorescence spectra of suramin in the absence and presence of excess C8 and C9, respectively. Significantly, the fluorescence of the drug was still enhanced by the proteins even in the presence of 0.5 M

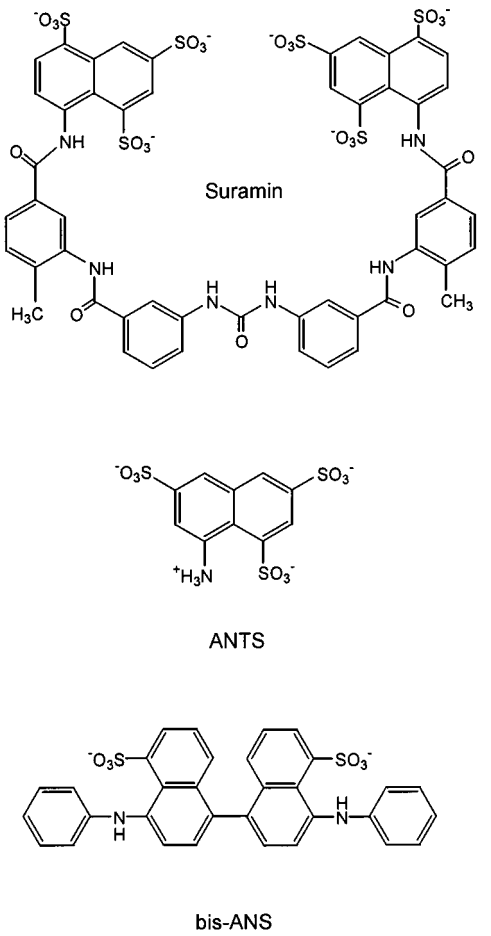

FIGURE 7: Structures of suramin, ANTS^{2-}, and bis-ANS^{2-}.

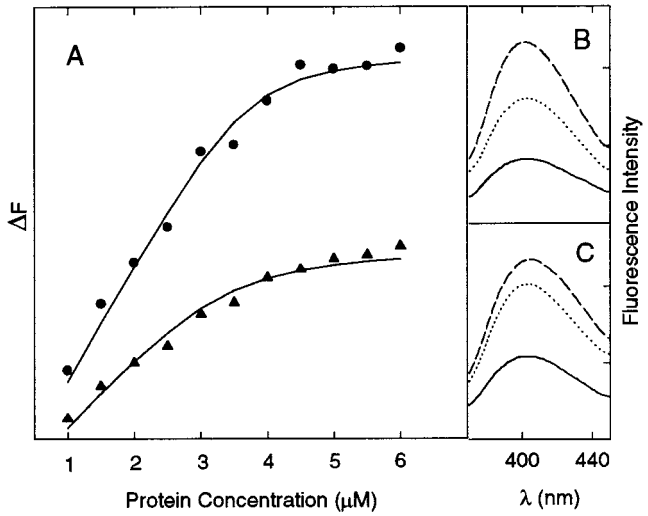

FIGURE 8: Fluorecence titration of suramin by C8 and C9. (A) Change in fluorescence intensity at 401 nm (ΔF) of 10 μM suramin in response to C8 addition (●) at 20 °C and C9 addition (▲) at 4 °C, respectively. (B) Emission spectra (dashed lines) of suramin in the presence of C8 in 10 mM Mops, 0.15 M NaCl, pH 7.2, or (C) in the presence of C9 in 10 mM Mops, 0.15 M NaCl, pH 7.2. The emission spectra of suramin in 0.5 M NaCl without (solid lines) and with the proteins (dotted lines) are also shown.

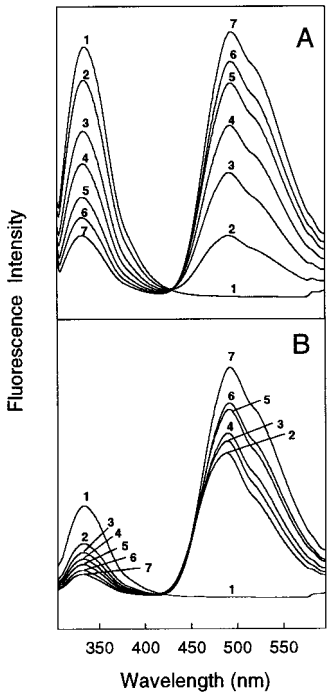

FIGURE 9: Fluorescence resonance energy transfer between the tryptophan residues in C8 and C9 and bound bis-ANS^{2-}. (A) Fluorescence of 1 μM C8 and (B) of 1 μM C9 with bis-ANS^{2-} at 0 μM (trace 1), 5 μM (trace 2), 10 μM (trace 3), 15 μM (trace 4), 20 μM (trace 5), 25 μM (trace 6), and 30 μM (trace 7). The excitation wavelength was 295 nm.

NaCl as shown by the dotted lines. Similar experiments performed with ANTS^{2-} gave no indication that this compound interacted with the proteins (not shown).

Because the separation of the fluorescence emission maxima of bis-ANS^{2-} and tryptophan is larger than between suramin and tryptophan, we used bis-ANS^{2-} to gain information on the binding sites of the drug. As shown in Figure 9 there was significant fluorescence resonance energy transfer (FRET) from tryptophans in C8 and C9 to bound suramin, indicating that they must be in close proximity.

Further insight into the binding mechanism was obtained by measuring oligomerization in the dependence of the drug concentration. It was conceivable that binding of suramin to one site on native C8 or C9 triggers a conformational change that causes unmasking of a second site required for oligomerization of the proteins. Alternatively, because of its bivalent nature, suramin could simply cross-link two molecules by binding to identical sites on each. If the latter mechanism were correct, then such dimers or trimers should revert back to monomers at high ligand concentration, that is, when all binding sites on each protein are occupied by a single suramin molecule. The Beckman XL-A centrifuge could not be used to monitor the stability of the protein complexes at high suramin concentrations because of its strong absorbance. For this reason we used MALLS to measure the fate of C9 dimers or C8 trimers in the presence of high concentrations of suramin. For these experiments freshly chromatographed monomeric C8 or C9 solutions were used and the MALLS instrument was used in batch mode to allow addition of suramin aliquots from a concentrated stock solution. A scintillation vial containing the protein solution was placed into the sample holder, but data were taken only

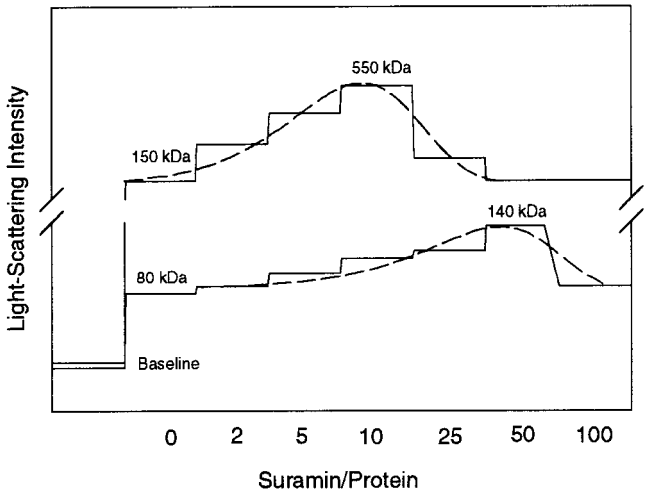

FIGURE 10: MALLS data of C8 and C9 in the presence of suramin. Light-scattering intensity changes of C8 (2 μM, upper trace) or C9 (1 μM, lower trace) in the presence of increasing amounts of suramin. Light scattering at 90° was recorded continuously after each stepwise addition of suramin, and the mass of the dominant species at the beginning and the maximum of each trace was calculated using data from all 18 angles and the Zimm formalism. The sample temperature was 27 °C.

Table 3: Suramin−Protein Affinities and Stoichiometry

protein	K_d (μM)	suramin/protein molar stoichiometry
C8	0.20 ± 0.04^a	$3.0^a/3.11^b$
C9	0.50 ± 0.09^a	$1.8^a/1.93^b$

[a] Calculated from Figure 8A using eq 1. [b] Determined by radial decomposition of suramin/protein absorbance contributions in sedimentation data using eq 2.

after the solution had reached thermal equilibrium at about 27 °C. As shown in Figure 10, the 90° light-scattering intensity increased with each addition of suramin, reaching a maximum at a molar ratio of 10 suramin/C8 or 50 suramin/C9 and then decreased again at higher concentrations. Quantitative analysis using data from all 18 angles and the Zimm formalism indicated that the mass (M_w) of C8 increased from 150 kDa in the absence of suramin to about 550 kDa, somewhat smaller than a tetramer, and then decreased again to the monomer state. In the case of C9 a much higher suramin concentration was required to reach the dimer state, but it also decreased again to the monomer at even higher suramin concentrations. Larger particles dominate light scattering, and the fact the apparent mass of the C8 sample increased to almost the tetramer M_w rather than the trimer seen in the ultracentrifuge may be indicative of this phenomenon.

Suramin−Protein Stoichiometry. The fluorescence titration curves shown in Figure 8A can be used to extract the stoichiometry of drug binding as well as the dissociation constant using eq 1. The solid lines shown in Figure 8A represent the fitted curves with values of $n = 2$ and $K_d = 0.50$ μM for C9 and $n = 3$ and $K_d = 0.20$ μM for C8 (Table 3). Suramin−protein-binding stoichiometries were also obtained from sedimentation equilibrium experiments. The radial distribution of the suramin−protein complexes was monitored in the ultracentrifuge at 315 nm (see Figure 5A), one of the absorbance maxima of suramin, and the stoichiometry was determined by radial decomposition of the

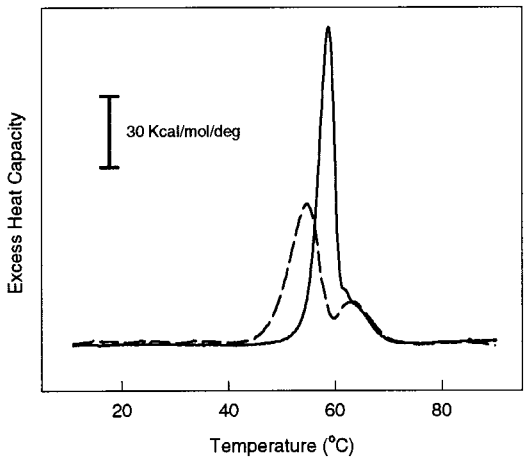

FIGURE 11: Influence of suramin on thermal denaturation of C8. DSC thermogram of C8 (25 μM) in 10 mM Mops, 0.15 M NaCl, pH 7.2, without (solid line) or with 125 μM suramin (dashed line). The scan rate was 30 °C/h, and all data were normalized for protein concentration.

absorbance according to eq 2. The calculated ratios (4 suramin/C9 dimer and 9 suramin/C8 trimer) are in complete agreement with the values obtained by fluorescence titration (Table 3). However, there was no evidence for suramin binding to C8 or C9 at 0.5 M NaCl; that is, the absorbance at 315 nm did not match the protein distribution monitored at 280 nm under these conditions (not shown).

Differential Scanning Calorimetry of C8. Because the van't Hoff plot for C8 trimerization was strongly biphasic with a distinct change in slope at 21 °C (Figure 6B), we searched for possible explanations for this behavior. Thus, differential scanning calorimetry was used to test for the possibility that the protein might undergo some kind of structural change at this temperature. Figure 11 shows the thermogram of C8 which can be deconvoluted into a major endothermic transition at 57 °C and two minor ones at 59 and 64 °C, respectively. The thermal unfolding of C8 was irreversible since no endotherm was present after rescanning (data not shown). Addition of suramin shifted the midpoint of the major transition from 57 to 51 °C and the 59 °C transition to 55 °C, respectively, indicating a slight destabilizing effect. Importantly, however, no protein transition could be detected at 21 °C.

DISCUSSION

The aim of our investigations is the characterization of the molecular interaction between terminal complement proteins in their native state and eventually a comparison of these interactions with those that occur during MAC assembly on a membrane. We have already described the association between C8 and C9 at physiologic ionic strength and at 12 °C using neutron scattering (*17*), but information about the affinity of the interaction was missing. It is now quite certain that native C9 and C8 bind to each other with moderate affinity (K_d = 0.6 μM at 20 °C) and specifically in the absence of any unfolding or refolding of the native proteins. When the interaction of the five terminal complement proteins in solution was described initially (*1*), it was suggested that the affinity between the native proteins was most likely too weak to be of significance in a physiological milieu because low ionic strength conditions were required to allow complex formation. At 37 °C the C8−C9 heterodimer dissociates with a K_d of 3.4 μM, indicating that indeed only a small percentage of the proteins may be associated since their serum concentrations are about 0.5 and 1.0 μM for C8 and C9, respectively. Of course, it will be important to measure the affinities of the other dimer pairs, that is, C5−C8, C5−C6, and C5−C6, and also of the pentamolecular C5,6,7,8,9 complex as precisely before a firm conclusion about the association state of the proteins in serum can be drawn. Nevertheless, the association between C9 and C8 was sufficiently strong at physiological ionic strength that thermodynamic values could be measured. The magnitude of the enthalpy and entropy values suggests that electrostatic interactions dominate the process (*26*). However, this interaction is most likely not only Coulombic in nature since the affinity between C9 and C8 in 0.15 M NaCl appears to be too high for a purely electrostatic interaction. For the illustration of this point, a one-to-one complex between an acidic protein, ovalbumin, and a basic protein, cytochrome *c*, has a dissociation constant of approximately 16 μM at 20 °C, pH 6.3, and a low ionic strength of 0.03 (*27*). Most likely such a dimer would not form in 0.15 M NaCl, but since there is no physiologic need for ovalbumin and cytochrome *c* to interact, it is not surprising that the interaction is governed by ion pair formation and lacks additional specificity. We obtained some indication for a more hydrophobic interaction of suramin with C8 and C9 because its fluorescence is still enhanced in 0.5 M NaCl where ionic interactions should be negligible. However, drug binding in high ionic strength must be weak because it could not be observed by sedimentation ultracentrifugation.

In any case our results demonstrate that the polyions suramin and protamine already block interaction between native C8 and C5 and between C8 and C9 and that uncovering of cryptic sites is not required. It is possible that the cationic site 1 on C9 shown in Figure 1 is involved in heterodimer formation and may be the binding site for suramin; however, at present we have no evidence for or against this possibility. What appears to be certain is that suramin prevents C8−C9 interaction by inducing protein oligomerization. Suramin binds to C8 and C9 with a submicromolar K_d but more strongly to C8 than to C9, and the C8 oligomers are about five times more stable than the C8−C9 heterodimers. Because the MALLS data indicate that C8 and C9 oligomers were dissolved by high concentrations of suramin, just like immune aggregates are dissolved at high antigen concentrations, it is likely that the drug causes cross-linking of the proteins. Although we have no evidence that the drug causes the proteins to unfold, which could lead to exposure of sites 2 and 3 in the Tschopp model (Figure 1), we cannot exclude the possibility that during the MAC assembly process suramin (and protamine) will bind also to these sites. As matter of fact it is quite likely that additional interactions are required since recent data by others indicate that the affinity of C9 for C8 in a membrane-bound C5b-8 complex is in the nanomolar range (*28*), that is, much stronger than the affinity of suramin for the native proteins. Future studies using isolated C9a and C9b fragments (*29*) should allow us to test whether binding of suramin and protamine to sites 2 and 3 is possible and also of importance for the inhibition of MAC assembly on a membrane.

The reason for the break at 21 °C in the van't Hoff plot for suramin-induced oligomerization of C8 is not clear. If there is a structural change in C8 at this temperature, then it is not associated with a significant heat capacity change since the DSC thermogram gave no indication for a phase transition. Interestingly, the prominent *negative* heat capacity change seen with C9 when it aggregates to poly(C9) at higher temperatures (*30*) was not observed with C8 in agreement with the known absence of poly(C8) formation. Suramin did, however, decrease the heat stability of C8 just as it did in the case of C9.

A further indication that suramin interacts not only with positively charged sites on C8 and C9 is the fact that $ANTS^{2-}$ has no affinity for C8 or C9. If suramin binding were purely electrostatic, one would expect that this molecule should bind likewise to the proteins and at least have some inhibitory effect on suramin-induced protein oligomerization. However, this was not the case. In this context it is useful to compare the binding of bis-ANS^{2-} and $ANTS^{2-}$ to other proteins with the binding of suramin to C8 and C9 or to the other proteins listed in the Introduction since such a comparison should provide information on the nature of suramin binding to C8 and C9. Much information is available on the binding of ANS^- to proteins since it has a long history as a fluorescent probe for protein structure in an aqueous milieu (*20*, *31*−*33*). Although we used $ANTS^{2-}$ and not ANS^- in our studies, we assume that the information gathered with ANS^- should be applicable to $ANTS^{2-}$. As was detailed by Matulis and Lovrien (*33*) the stoichiometry of ANS^- binding is largely determined by the sulfonate group and the number of cationic groups provided by the target proteins, and these proteins do not need to have large hydrophobic patches. Dissociation constants for protein-bound ANS^- are frequently in the high micromolar range, but only a few of the bound ANS^- molecules fluoresce. ANS^- fluorescence production is sharply dependent on the absence of fluorescence quenching water molecules around the bound ligand and therefore is a consequence of the structure of the ligand−protein complex and not a property of the initial protein. Proteins which do have binding pockets that can accept hydrophobic ligands such as the intestinal fatty acid-binding protein (iFABP) bind ANS^- a bit more tightly ($K_d \approx 10\ \mu M$) and the stoichiometry of ANS^- binding to iFABP is one; that is, binding is strictly dependent on the number of cationic sites in the binding pocket (*20*, *33*). The fact that $ANTS^{2-}$ does not bind strongly to C8 and C9 but suramin and bis-ANS^{2-} do indicates that the organic moiety and the bivalent nature of the latter are of importance in the binding process. Binding causes strong fluorescence enhancement of suramin and of bis-ANS^{2-}, which makes it likely that they reside in protein pockets that exclude free water molecules. Furthermore, it is important to note that all bound molecules are fluorescent since binding stoichiometries measured by absorbance (i.e., sedimentation equilibrium centrifugation) agree with those measured by fluorescence titration (Table 3).

The fluorescence enhancement and the fluorescence resonance energy transfer from tryptophans to bis-ANS^{2-} argue against a model for the suramin−protein complexes in which the drug forms a mere bridge between adjacent protein molecules with the aromatic rings exposed to water. However, it is difficult to construct a detailed model of the suramin−protein oligomers that would satisfy the observed stoichiometries between the drug and C8 and C9 and the observation that $ANTS^{2-}$, even at high concentration, did not compete with suramin whereas high excess suramin caused dissociation of the protein oligomers. It is well-established that suramin binds to growth factors (*14*), suggesting that the EGF domain present in C8α, C8*β*, and C9 could contain the suramin-binding pocket. However, in many of these cases the drug/protein stoichiometry was one, whereas oligomers of C9 bound two suramin per protein monomer and C8 bound three. We have not attempted to calculate fluorescence donor−acceptor distances using the Förster formalism because there are four and nineteen tryptophans in C9 and C8, respectively, and more than one suramin molecule was bound per protein monomer, making it highly unlikely that meaningful distances could be obtained. Again future studies with isolated C9α and C9*β* and C8α and C8*β* should be useful in providing more precise molecular details.

ACKNOWLEDGMENT

We are grateful to Peter Schuck for assistance in sedimentation equilibrium data analyses, Jarmilla Janatova for human C5, and the Bayer Company for providing suramin and Cohn Fraction III.

REFERENCES

1. Kolb, W. P., Haxby, J. A., Arroyave, C. M., and Müller-Eberhard, H. J. (1972) *J. Exp. Med. 135*, 549−566.
2. Stewart, J. L., Kolb, W. P., and Sodetz, J. M. (1987) *J. Immunol. 139*, 1960−1964.
3. Stewart, J. L., and Sodetz, J. M. (1985) *Biochemistry 24*, 4598−4602.
4. Bhakdi, S., and Tranum-Jensen, J. (1984) *J. Immunol. 133*, 1453−1463.
5. Bhakdi, S., and Tranum-Jensen, J. (1986) *J. Immunol. 136*, 2999−3005.
6. DiScipio, R. G., Chakravarti, D. N., Müller-Eberhard, H. J., and Fey, G. H. (1988) *J. Biol. Chem. 263*, 549−560.
7. Tschopp, J., and Masson, D. (1987) *Mol. Immunol. 24*, 907−913.
8. Brown, M. S., Deuel, T. F., Basu, S. K., and Goldstein, J. L. (1978) *J. Supramol. Struct. 8*, 223−234.
9. Stanley, K. K., and Herz, J. (1987) *EMBO J. 6*, 1951−1957.
10. Tschopp, J., Masson, D., Schäfer, S., Peitsch, M., and Preissner, K. T. (1988) *Biochemistry 27*, 4103−4109.
11. Götze, O., Haupt, I., and Fischer, H. (1968) *Nature 217*, 1165−1167.
12. Levine, A. M., Gill, P. S., and Cohen, J. (1986) *Ann. Intern. Med. 105*, 32−37.
13. Stein, C. A., La Rocca, R. V., and Thomas, R. (1989) *J. Clin. Oncol. 7*, 499−508.
14. Middaugh, C. R., Mach, H., Burke, C. J., Volkin, D. B., Dabora, J. M., Tsai, P. K., Bruner, M. W., Ryan, J. A., and Marfia, K. E. (1992) *Biochemistry 31*, 9016−9024.
15. Cadene, M., Duranton, J., North, A., Si-Tahar, M., Chignard, M., and Bieth, J. G. (1997) *J. Biol. Chem. 272*, 9950−9955.
16. Polenova, T., Iwashita, T., Palmer, A. G. I., and McDermott, A. E. (1997) *Biochemistry 36*, 14202−14207.
17. Esser, A. F., Thielens, N. M., and Zaccai, G. (1993) *Biophys. J. 64*, 743−748.
18. McGuire, J. J., and Haile, W. H. (1996) *Arch. Biochem. Biophys. 335*, 139−144.
19. Esser, A. F., and Sodetz, J. M. (1988) *Methods Enzymol. 162*, 551−578.
20. Kirk, W. R., Kurian, E., and Prendergast, F. G. (1996) *Biophys. J. 70*, 69−83.

21. Johnson, M. L., Correia, J. J., Yphantis, D. A., and Halvorson, H. R. (1981) *Biophys. J. 36*, 575−578.
22. Durchschlag, H. (1986) in *Thermodynamic data for biochemistry and biotechnology* (Hinz, H. J., Ed.) pp 45−128, Springer-Verlag, New York.
23. Laue, T. M., Shah, B. D., Ridgeway, T. M., and Pelletier, S. L. (1992) *Analytical Ultracentrifugation in Biochemistry and Polymer Science* (Harding, S., Rowe, A., and Horton, J. C., Eds.) pp 90−125, Royal Society of Chemistry, London, U.K.
24. Lewis, M. S., Carmassi, F., and Chung, S. I. (1984) *Biochemistry 23*, 3874−3879.
25. Wyatt, P. J. (1993) *Anal. Chim. Acta 272*, 1−40.
26. Ross, P. D., and Subramanian, S. (1981) *Biochemistry 20*, 3096−3102.
27. Winzor, D. J., Jacobsen, M. P., and Wills, P. R. (1998) *Biochemistry 37*, 2226−2233.
28. MacKay, S. L., and Dankert, J. R. (1994) *Infect. Immun. 62*, 2800−2805.
29. Shiver, J. W., Dankert, J. R., Donovan, J. J., and Esser. A. F. (1986) *J. Biol. Chem. 261*, 9629−9636.
30. Lohner, K., and Esser, A. F. (1991) *Biochemistry 30*, 6620−6625.
31. Daniel, E., and Weber, G. (1966) *Biochemistry 5*, 1893−1900.
32. Slavik, J. (1982) *Biochim. Biophys. Acta 694*, 1−25.
33. Matulis, D., and Lovrien, R. (1998) *Biophys. J. 74*, 422−429.

BI990040J